

## Chapter 6

### ***In Vitro* and *In Silico* Interaction of Faba Bean (*Vicia faba* L.) Seed Extract with Xanthine Oxidase and Evaluation of Antioxidant activity**

---

#### **6.1. Introduction**

Faba bean (*Vicia faba* L.) is an annual legume botanically known as *Vicia faba* L. (Hanelt and Mettin, 1989). Faba bean was generally named as broad bean, horse bean and field bean comes under the family of *Fabaceae*. It is grown as winter and summer crop in Mediterranean areas and other regions of Europe and South America and is one of the most vital plant food material for the Nile River populations (Amarowicz and Pegg, 2008). It is exploited in folk medicines such as anti-hyperlipidemic to control cholesterol (Bouchenak and Lamri-Senhadji, 2013; Mulvihill and Huff, 2010; Rabey et al., 1993). *Vicia faba* L. flowers are also reported as lipase and a melanogenesis inhibitor and may be a potential use for it as a skin whitening agent (Allam et al., 2017). Gout and metabolic syndromes like diabetes mellitus are due to abnormal xanthine oxidase (XO) activity and high serum uric acid concentrations results (Ferreira Antunes et al., 2016; Song et al., 2016). Many bioactive components of plants on XO regulation and serum uric acid concentrations are being already studied in gout-disease models (Gao et al., 2017; Guo et al., 2003; Nile and Park, 2015; Tang et al., 2016; Wan et al., 2016). One remedy for acute arthritis (gout) is the exploit of xanthine oxidase inhibitors such as artificial drug allopurinol (Emmerson, 1996). Xanthine oxidase is inhibited by drug allopurinol but that is cost effective and has more side effects. Therefore, we selected faba bean (*Vicia faba* L.) polyphenols for suppression of xanthine oxidase by the *in vitro* and *in-silico* method. The major cause that has delayed research on polyphenols is due to complexity or diversity of their chemical structures. That is the reason the motivation behind this

*School of Biochemical Engineering, IIT(BHU) Varanasi*

investigation was to investigate the antioxidant activity of faba bean seed extract and *in silico* interaction with xanthine oxidase.

## **6.2. Experimental**

### **6.2.1. Seed Material and their characterization**

Details about faba beans seed have already discussed in Chapter 3. Extraction, purification, and characterization of faba beans have mentioned in chapter 3.

#### **6.2.1. Chemicals**

Diphenyl-1-picrylhydrazyl (DPPH), gallic acid, sodium carbonate, folin–Ciocalteu reagent, quercetin, sodium hydroxide, 2,2- ascorbic acid, polyphenols standard, and other HPLC solvents were purchased from Merck and HiMedia, Mumbai. Allopurinol was purchased from a medical store. Bovine milk xanthine oxidase was procured from Sigma–Aldrich, Mumbai, India. Experimental chemicals were utilized as a pure analytical grade.

#### **6.2.3. Total phenolics content**

The total phenolic content of the crude seed extract was evaluated according to the method described by (Singleton and Rossi, 1965). 1 mg/ml of different samples were taken in test tubes and by dilution with the same solvent up to 10 ml. Different concentrations of samples were taken in different test tubes. This same procedure was used for the standard. 1ml of Folin–Ciocalteu reagent was added in this concentration and the content of the flask was mixed thoroughly and 10 min later, 4 ml of 20% sodium carbonate was added, and the mixture was allowed to stand for 30 min with intermittent shaking. The absorbance of the blue color that developed was read at 765 nm in UV spectrophotometer.

#### **6.2.4. Determination of total flavonoid content**

Aluminum chloride colorimetric test was used for determination of total flavonoid content. 1 ml standard quercetin solution (0.1, 0.2, 0.4, 0.6, 0.8, 1 mg/ml) and 1ml of aliquots were kept into series of test tubes. 4 ml of distilled water and 0.3 ml of 5 % sodium nitrite solution was added. 0.3 ml of 10 % aluminum chloride and 2 ml of 1 M sodium hydroxide was included one by one with some time intervals. Samples were vortexed and volume maintained up to 10 ml. A calibration curve was plotted by using quercetin as a standard at absorbance by 540 nm. The total flavonoid content was expressed by mg of quercetin equivalents/gm of dry weight.

### **6.2.5. *In vitro* antioxidant activity**

DPPH free radical scavenging assay, phenolics content by Folin–Ciocalteu reagent and estimation of reducing power were performed by Oyaizu (Oyaizu, 1986) for the determination of potential antioxidant activity of seed extracts.

#### **6.2.5.1. DPPH scavenging assay**

The free radical scavenging ability of the acetone and methanol seed extract was evaluated by using DPPH method (An et al., 2008). Percent scavenging of the DPPH free radical was calculated in the following term:  $I \% = 100 (A_{\text{blank}} - A_{\text{sample}})/A_{\text{blank}}$ . Such as,  $A_{\text{blank}}$  is the absorbance of the control reaction (containing all reagents except the test compound), and  $A_{\text{sample}}$  is the absorbance of the test compound.

### **6.2.6. *In vitro* xanthine oxidase inhibitory activity**

*Vicia faba* seed extracts were assayed for their *in vitro* xanthine oxidase inhibitory action. The xanthine oxidase inhibitory activity evaluation was based on the procedure and described by (Owen and Johns, 1999). Xanthine as substrate, (0.1 mL) xanthine oxidase enzyme solution (0.1 units/mL in phosphate buffer, pH 7.5), 2.9 mL of phosphate buffer (pH 7.5) and, 1 mL of the seed extract (5-100 µg/mL) was mixed. First, it was kept for preincubation at 25°C for 15 min and before 150 mM xanthine in the same buffer was

added. The assay mixture was then incubated at 25 °C for 30 min. The reaction was stopped by the addition of 1 mL of 1 N hydrochloric acids and the absorbance was measured at 290 nm (Yu et al., 2006),(Nguyen et al., 2005). Seed extract (5-100 µg/mL) were dissolved in dimethyl sulfoxide (DMSO) and the final concentration of DMSO was made up to 5 %. Allopurinol (5-100 µg/mL), an outstanding inhibitor of xanthine oxidase, was used as the positive control for this above assay protocol. Xanthine oxidase inhibitory activity was expressed as the percentage inhibition of xanthine oxidase by crude seed extract in the above assay procedure calculated as this formula : (% I (inhibition) =  $(1 - [B/A]) \times 100$ . The mode of inhibition was determined by the Lineweaver-Burk plot using varying concentrations of xanthine.

#### **6.2.7. Statistical analysis**

All experimental method were performed in 3 different sets with each set in triplicates. These data were represented as mean  $\pm$  SD. Values of  $p \leq 0.05$  which were considered as statistically significant.

#### **6.2.8. *In silico* studies**

##### **6.2.8.1. Preparation of protein**

The three-dimensional (3D) structure of (PDB ID: 1FIQ) of xanthine oxidase from bovine milk was recovered from RCSB protein data bank. Chimera 1.10.2 (Pettersen et al., 2004) was used for energy minimization purpose.

##### **6.2.8.2. Selection of ligands**

Based on literature (Aqil et al., 2006), HPLC analysis, chemo-profiling (Chapter 3), it was found that the dynamic constituents of *Vicia faba* seed extract *i.e.* phenolics (Gallic acid, Ellagic Acid, Catechin, Epicatechin) were chosen. Allopurinol was selected as a reference molecule.

##### **6.2.8.3. Molecular drug-likeness properties predictions**

*School of Biochemical Engineering, IIT(BHU) Varanasi*

All ligand molecules were analyzed for their molecular drug properties such as Lipinski's Rule of Five), the drug-likeness score was predicted using PreADMET server (Lee et al., 2003) (**Table 6.1**). The motivation behind this current Lipinski's Rule of Five distinguishes between the drug like and non-drug like molecules (Lipinski et al., 1997).

**Table 6.1:** Drug-likeness prediction of polyphenols and allopurinols

Compounds	CMC like rule	Lead like rule	Rule of five	WDI like rule	MDDR like rule
Gallic acid	Not qualified	Violated	Suitable	Out of 90% cut off	2 (violated)
Ellagic acid	Qualified	Suitable if its binding affinity is greater than 0.1 micro M	Suitable	In 90% cut off	1
Catechin	Qualified	Suitable if its binding affinity is greater than 0.1 micro M	Suitable	In 90% cut off	1
Epicatechin	Not qualified	Not qualified	Suitable	In 90% cut off	3 (Non drug- like)
Allopurinol	Not qualified	Violated	Suitable	In 90% cut off	Non-drug-like

Polyphenols represent gallic acid, ellagic acid, catechin and epicatechin.

According to that rule when ligand or drug takes after into following criteria for drug resemblance: number of hydrogen bond donors  $\leq 5$  (The aggregate of OHs and NHs), number of hydrogen bond acceptor  $\leq 10$  (The sum of Os and Ns) and molecular weight  $\leq 500$  and CLogP  $\leq 5$  ( $M \log P \leq 4.5$ ).

#### **6.2.8.4. Ligand preparation**

Three -dimensional structures of different ligands were retrieved from PubChem Compound information base. The ID of differently selected ligands were as follows for example, Gallic acid [CID370], Ellagic Acid [5281855], Allopurinol [CID2094], Catechin [CID73160], Epicatechin [CID3084390], Their energy forms minimization was done by pyRX virtual screening tool (Dallakyan and Olson, 2015) and they were changed to PDB format by the Open Babel 2.3.1.(O'Boyle et al., 2011).

#### **6.2.8.5. Molecular docking**

The Ellagic Acid [5281855], Allopurinol [CID2094], Catechin [CID73160], Epicatechin [CID3084390], catechin [CID73160] and gallic-acid [CID370] compounds (Figure1) were docked on the crystal structure of XO (PDB ID: 1FIQ) (Abu-Reidah et al., 2015) using AutoDock 4.2 (Morris et al., 2009). The numbers of grid points in x, y, z were set to 70,70, 70 with the spacing value equivalent to 0.375 Å. Blind docking was performed having 150 runs and . AutoDock handles the Lamarckian genetic algorithm (LGA) to search for the best conformers .The population in the genetic algorithm was 50, the number of energy evaluations was 250,000, and the maximum number of iterations was 27,000. Other parameters were set at the default values implemented by the program. Further interaction analysis was done using the autodock tools and imagined by the Chimera1.10.2 and LigPlot+(v.1.4.5) (3D to 2D) (Laskowski and Swindells, 2011).

#### **6.2.8.6. Molecular dynamics simulation**

##### **6.2.8.6.1. System building**

GROMACS 4.6.7 packages (Pronk et al., 2013; Van Der Spoel et al., 2005) were used for preparing the system and performing MD simulations using the gromos53a6 force field (Oostenbrink et al., 2004). The protein solute was solvated by explicit SPC216 water (Toukan and Rahman, 1985) in a dodecahedron box with a margin of 10 Å between solute and the box walls. Systems were brought to neutrality by addition of sodium counter ions.

#### **6.2.8.6.2. Simulation detail**

1 nm cut-off distance was taken under the particle-mesh Ewald method (Essmann et al., 1995) to calculate long-range electrostatic interactions and 1nm cut-off distance was also considered to evaluate van der Waals interactions. The LINCS algorithm of fourth order expansion was used to constrain bond lengths (Hess et al., 1997). The steepest-descent algorithm was applied to optimize for 10,000 steps to remove steric clashes between atoms. The system was equilibrated for 1ns with position restraints of all heavy atoms. Berendsen weak coupling schemes were used to maintain the system at 300 K and 1 atm using separate baths for the system. Initial velocities were generated randomly using a Maxwell-Boltzmann distribution corresponding to 300 K. Every 10 fs using a group cut-off scheme was set for updating neighbor lists. Finally, the production run was performed for 20 ns. Furthermore, xmgrace (<http://plasma-gate.weizmann.ac.il>) was used for preparing graphs. PyMol (**The PyMOL Molecular Graphics System, Version 1.7 Schrödinger, LLC**) packages were applied for a system inspection. Moreover, ligand topology preparation was implemented by using the PRODRG server with the option of choosing no chirality, full charge and no energy minimization (Schüttelkopf and Van Aalten, 2004).

#### **6.2.8.6.3. Trajectory analysis**

The `g_rms` tool of the GROMACS package was used to calculate the root mean square deviation (RMSD) of each trajectory. The equilibrated structure obtained after equilibration was considered as the reference structure and the trajectories were fitted to the backbone of this structure. Temporal distribution was approximated using the `g_cluster` tool.

### 6.3. Results and Discussion

#### 6.3.1. Total phenolic content

The total phenolics content of acetone and ethanol extract of *Vicia faba* seed was calculated as gallic acid equivalent. It is evident from (Figure 6. 1 ), that maximum phenol content was observed in the case of acetone extract(33.87±0.70 gallic acid equivalent/gm dw). Phenols are very important plant constituents because of their scavenging ability due to their hydroxyl groups.

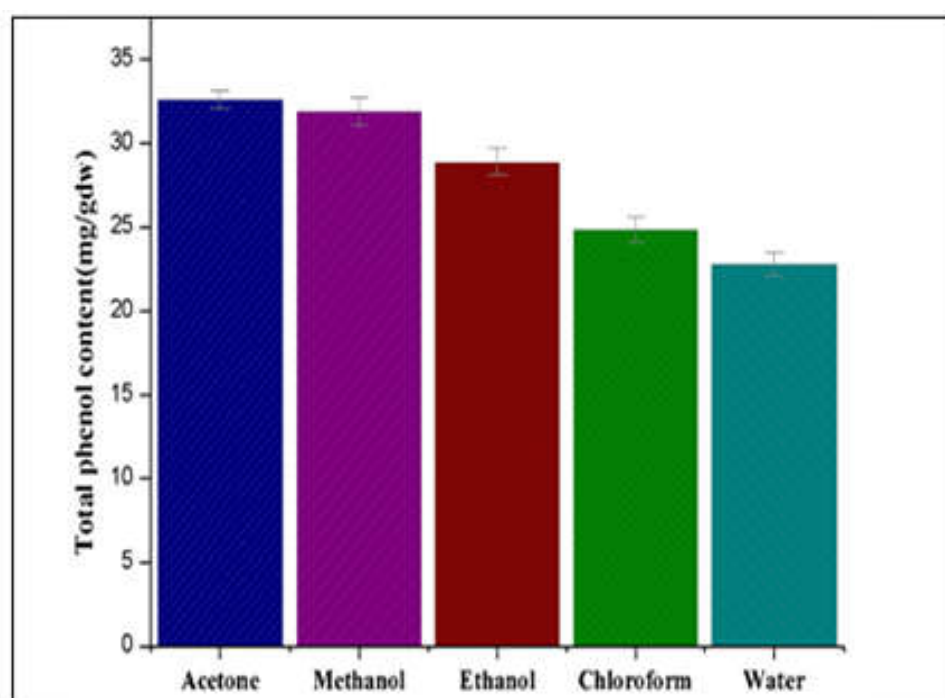


**Figure 6.1.** Total phenolic content of *Vicia faba* seed extracts (mg/dry weight) in a different solvent (acetone, methanol, ethanol, water, chloroform).



### 6.3.2. Total flavonoid content

The total phenolics content of acetone and ethanol extract of *Vicia faba* seed was calculated as quercetin equivalent. Maximum flavonoid content was found in acetone extract ( $27.93 \pm 0.45$  quercetin equivalent/gm dw) (**Figure 6.2**).

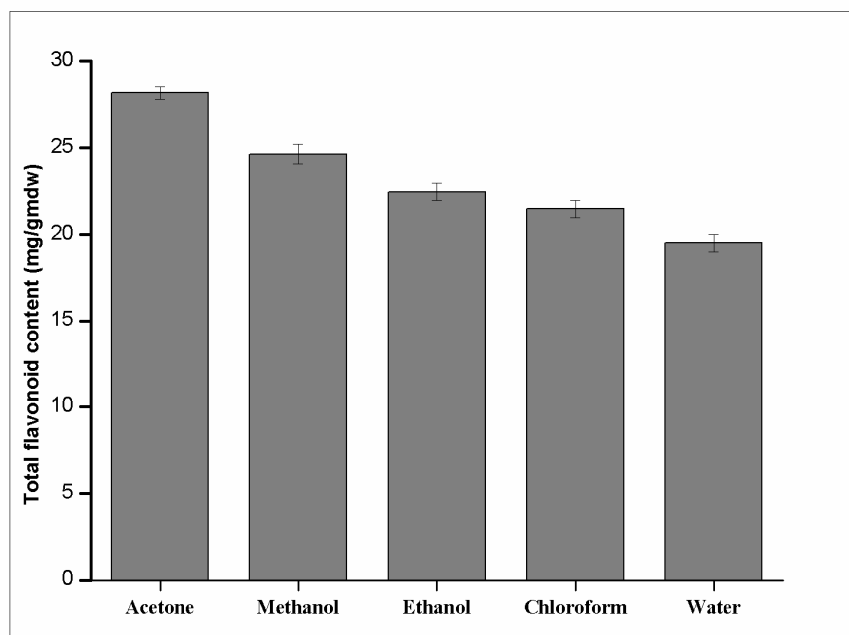


**Figure 6.2.** Total flavonoid content of *Vicia faba* seed extracts (mg/dry weight) in a different solvent (acetone, methanol, ethanol, chloroform, water)

### 6.3.3. DPPH scavenging assay

Again from the (**Figure 6.3**), it was observed that ascorbic acid at a concentration of 10  $\mu\text{g/mL}$  exhibited percentage inhibition of 45.63% and concentration of 50  $\mu\text{g/mL}$  was 97.36%. Similarly, acetone and methanol extract exhibited maximum percentage inhibition at concentration 50  $\mu\text{g/mL}$  was 86.47 % and 74.69 % respectively (**Figure 6.3**), it was confirmed that both extracts had significant DPPH radical scavenging activity.  $\text{IC}_{50}$  value of ascorbic acid was found to be 9  $\mu\text{g/mL} \pm 0.20$  and in the case of acetone extract, it

was found to be  $30 \mu\text{g/mL} \pm 0.21$  (Table 6.2). Much attention is now being paid on the antioxidant capacity of the flavonoids and the phenolics (Kumar et al., 2015). Studies made by others also authenticate that there is an extremely positive relationship between total phenolic content and antioxidant activity in many plant species. (Duh et al., 1999),(Gülçin et al., 2004).

**Table 6.2:** Different extracts of  $\text{IC}_{50}$  values with respect to standard (Ascorbic acid).

S.no	Extracts	$\text{IC}_{50}$ values
1	Acetone	$30 \mu\text{g/ml} \pm 0.21$
2	Methanol	$40 \mu\text{g/ml} \pm 0.23$
3	Ethanol	$55 \mu\text{g/ml} \pm 0.26$
4	Water	$120 \mu\text{g/ml} \pm 0.25$
5	Chloroform	$205 \mu\text{g/ml} \pm 0.28$
6	Ascorbic acid	$9 \mu\text{g/ml} \pm 0.20$

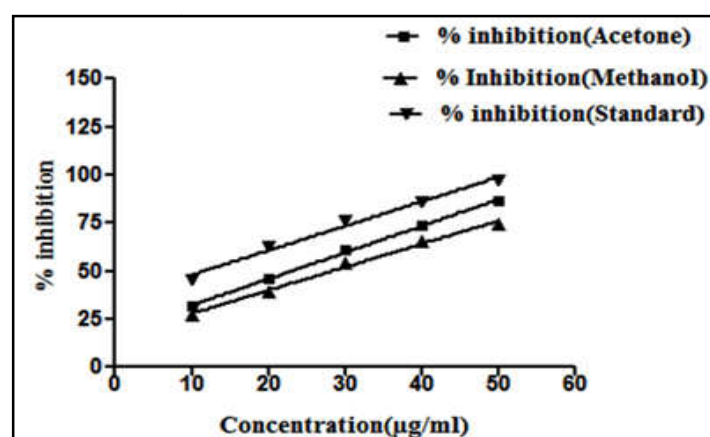


**Figure 6.3.** Free radical scavenging activity in terms of percentage inhibition of acetone and methanol extract extracts with respect to standard (ascorbic acid)

*School of Biochemical Engineering, IIT(BHU) Varanasi*

### 6.3.4. Reducing power

Reducing power depends upon on the rule that any substances or chemicals which have reduction capability respond with potassium ferricyanide ( $\text{Fe}^{3+}$ ) to form potassium ferrocyanide ( $\text{Fe}^{2+}$ ), which at that point responds with ferric chloride to form ferric-ferrous complex that has an absorption maximum at 700 nm monitored by measuring the formation of Pearl's Prussian blue (**Figure 6.4**) showed that how the reducing power of the test extracts increased with the increase in amount of sample. Antioxidant activity outcome is correlating with reductive activity (Duan et al., 2006) as shown in the literature.

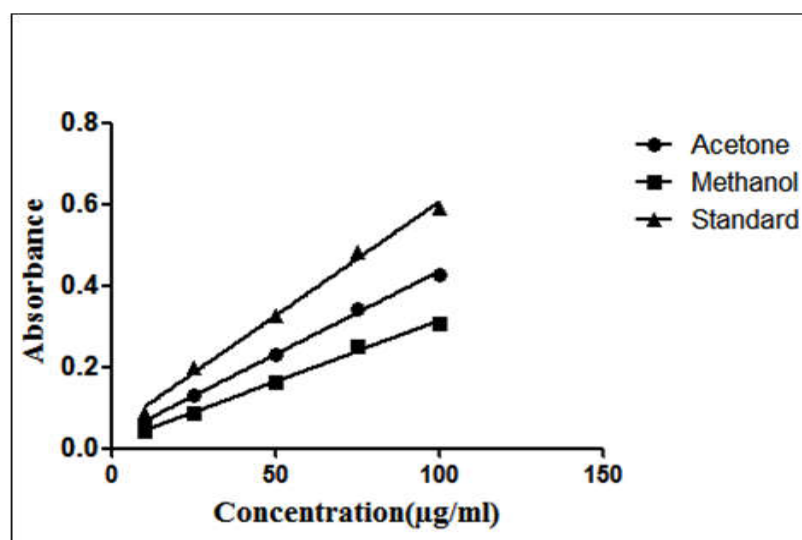


**Figure 6.4.** The absorbance of various concentrations ( $\mu\text{g/mL}$ ) of standard (ascorbic acid) and seed extracts in ferric reducing power

### 6.3.5. *In vitro* xanthine oxidase inhibitory activity

It was obvious from (**Figure 6.5**) that the mode of xanthine oxidase inhibition by the seed extract is of mixed type (between the uncompetitive and noncompetitive type of

inhibition). The *in vitro* inhibition of xanthine oxidase by the seed extract was found to be lesser than allopurinol (**Figure 6.5**). There have been no studies or reports in our knowledge recently regarding inhibition of xanthine oxidase inhibition activity by faba bean seed extract, but few seed, plant, vegetable flower, the flavor had xanthine oxidase inhibition activity (Ong et al., 2017).

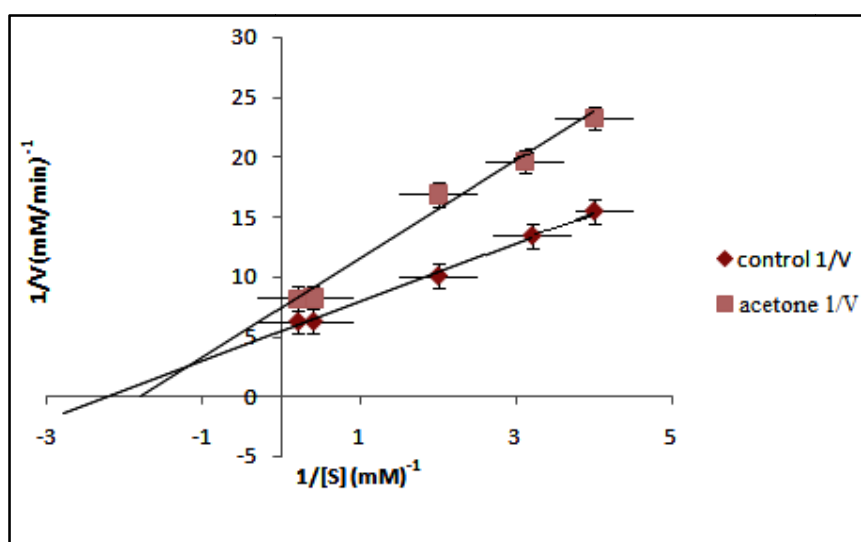


**Figure 6.5.** Lineweaver–Burk plot showing mixed inhibition of acetone extract with respect to control

### 6.3.6. Molecular docking studies

On the basis of *in vitro* studies of polyphenols with xanthine oxidase, it was further validated by *in silico* study by using that gallic acid, ellagic acid, catechin, epicatechin (polyphenols). Literature suggests that interacting catalytic binding sites of xanthine oxidase is Glu-1261. The docked most stable confirmation showed binding energy in the range of  $-4.94$  to  $-7.74$  Kcal/mol. (**Table 6.2**).

**Table 6.2:** Docking analysis of different ligands with xanthine oxidase compare with allopurinol.

Compounds	Binding energy(kcal/mol)	Hydrogen bond	Crucial amino acid
Allopurinol	-4.94	1	Lys 1127
Gallic acid	-6.39	5	Lys1127,Ser1124,Arg367,Gln367, Lys374
Catechin	-7.78	2	Glu1109,Lys1127
Epicatechin	-6.11	2	Ile1128, Lys 1127
Ellagic acid	-5.78	4	Ala279,Gly46,Ile1128,Ser1133

It was demonstrated that the catechin exhibits binding energy of  $-7.78$  kcal/mol and allopurinol as a standard drug exhibits binding energy of  $-4.94$  Kcal/mol. Standard drug allopurinol displayed hydrogen binding with amino acid residues, Lys 1127 (**Figure 6.6 (a)**). It binds other than the catalytic residue of xanthine oxidase. Allopurinol, a structural analog of xanthine is the best-known inhibitor of xanthine oxidase Allopurinol is converted to oxypurinol in the catalytic center of xanthine oxidase. Allopurinol at low concentration binds competitively but at high concentration binds non competitively. Both compounds compete with the physiological substrates for the active center of the enzyme. Once oxypurinol has formed a complex with the enzyme, it dissociates very slowly from the active center of the enzyme. Oxypurinol is a very competent tight-binding inhibitor of xanthine oxidase and exerts non-competitive type inhibition (Costantino et al., 1992). Literature supporting evidence and docking studies authenticated that enzyme followed mixed type inhibition in the presence of standard and test compound. Lig plot analysis confirmed that gallic acid having binding energy ( $-6.39$  Kcal/mol) and exhibiting hydrogen bonding with amino acid residues

Lys1127, Ser1124, Arg367, Gln367, Lys374 (**Figure 6.6(b)**), catechin having binding energy (-7.78 Kcal/mol) showed hydrogen bonding with amino acid residues Glu1109, Lys1127 (**Figure 6.6(c)**), epicatechin with Ile1128, Lys 1127 (**Figure 6.6(d)**) and ellagic acid binds having hydrogen bonding with Ala279, Gly46, Ile1128, Ser1133 (**Figure 6.6 (e)**). The studies made by worker were primarily focussed on only antioxidant activity of seed extract. Therefore, an attempt was made to establish the interaction of polyphenols with xanthine oxidase by *in silico* study.

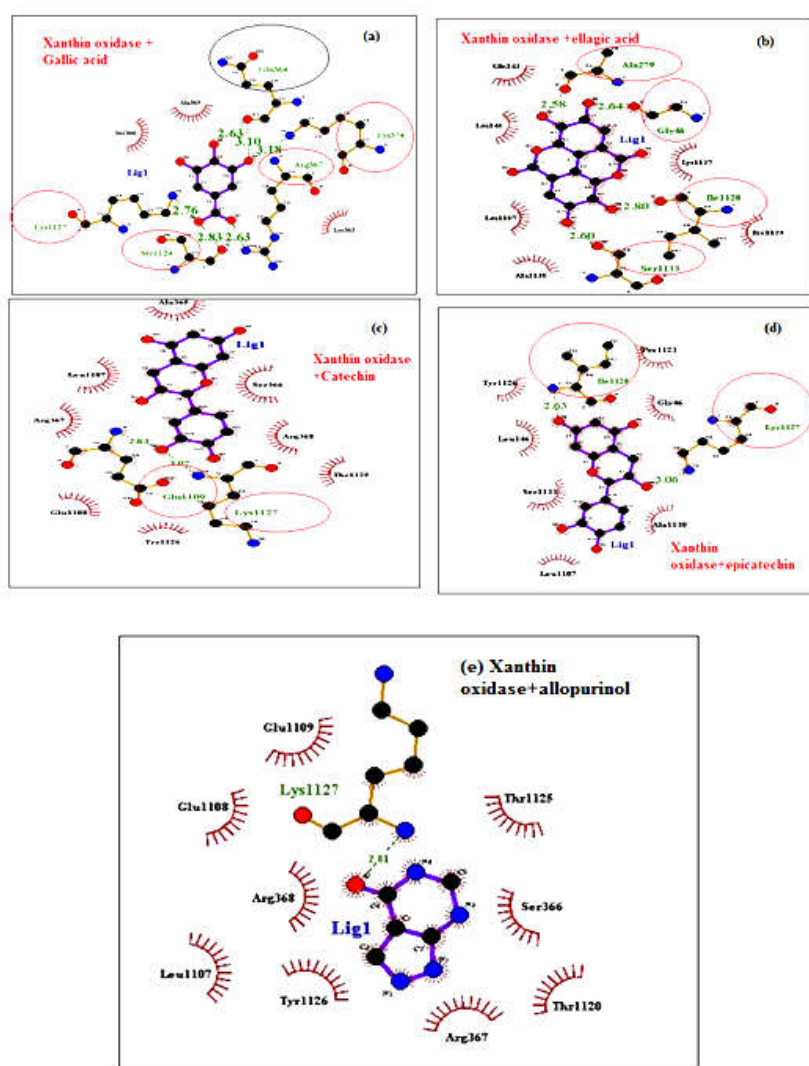


**Figure 6.6.** Lig plot showing the interaction between (a) allopurinol and xanthine oxidase, (b) catechin and xanthine oxidase (c) epicatechin and xanthine oxidase (d) ellagic acid and xanthine oxidase (e) gallic acid and xanthine oxidase.

### 6.3.7. Molecular dynamics simulation

The simulation was carried out for 10 ns for the apo state of XO whereas holo: XO was simulated for total of 20 ns. **Table 6.3** reports the simulations performed in this study. Each of the simulations was initiated with randomly selected initial velocities.

**Table 6.3:** List of system and simulations detail.

System	Ligand	PDB file	Duration (ns)	Repeats
Apo: XO	Nil	1FIQ	10	1
Cat:XO	Catechin	1FIQ	20	1
Gal: XO	Gallic acid	1FIQ	20	1

#### 6.3.7.1. Root mean square deviation

The total 20-ns trajectory was used for analyses; consequently, we observed catechin (red line plot **Figure 6.7**) was found stable and was observed to remain strictly within the binding pocket at the end of the simulation. On the contrary, RMSDs of gallic-acid (blue line plot **Figure 6.7**) shows high fluctuations signify the insignificant movement of gallic-acid during the simulation; however, the movement occurred within the binding pocket. To evaluate the quality of complexes including the apo state of the enzyme, the RMSD values of the protein backbone atoms relative to the initial equilibrated structure during the phase of the simulation were calculated (sub-plot **Figure 6.7**).

Each system reached equilibrium after ~8-ns of the simulation phase and remained similar pattern till end of the simulation. In addition, the result shows that the

*School of Biochemical Engineering, IIT(BHU) Varanasi*

trajectories of the MD simulations for both complexes after equilibrium were reliable for post analyses. Apo-state of the enzyme (10-ns simulation) exhibits the same pattern RMSD fluctuated within  $\sim 0.18$ -nm to  $\sim 0.23$ -nm. Holo-state complexes were exhibited approx same pattern after 10-ns which suggesting a conformational change during MD simulation.

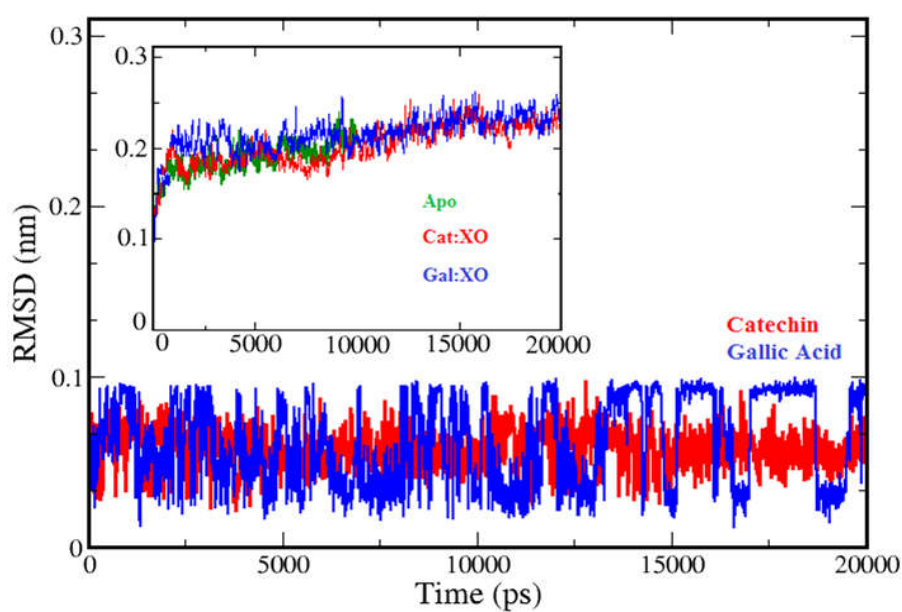


**Figure 6.7.** Backbone atom Root mean square deviation calculations (RMSDs) of catechin and gallic-acid compound (red and blue respectively) are approximated. Further, the RMSDs of each complex system is also depicted in the subplot. Green, red and blue color code is assigned for apo (10-ns), Cat: XO and Gal: XO respectively.

### 6.3.7.2. Cluster analysis

The trajectories were subjected to cluster analysis (cut-off value 0.15-nm) to secure convergence, as well as observe the effect of both ligands during simulation. As figure 18 reports, the large dominating clusters which were appeared in reduced equilibrium with almost full lifetime structures. This observation was elaborated as the system is sampled hardly single conformation that obviously, will not differ from their



stability. For complex Cat: XO, initially there were found  $\sim 7$  clusters, although, at the later simulation time, it resists up to  $\sim 1$  to 2 clusters which show longer lifetime (bold arrow **Fig 6.8**). However, one cluster was possessed comparatively longer time ( $\sim 14$ -ns) and we have recruited a representative structure that belongs to the largest cluster. At the beginning of the simulation, maximum clusters for Gal: XO complex were classified up to 5 clusters, after  $\sim 5$ -ns time, it is acquired 2 leading

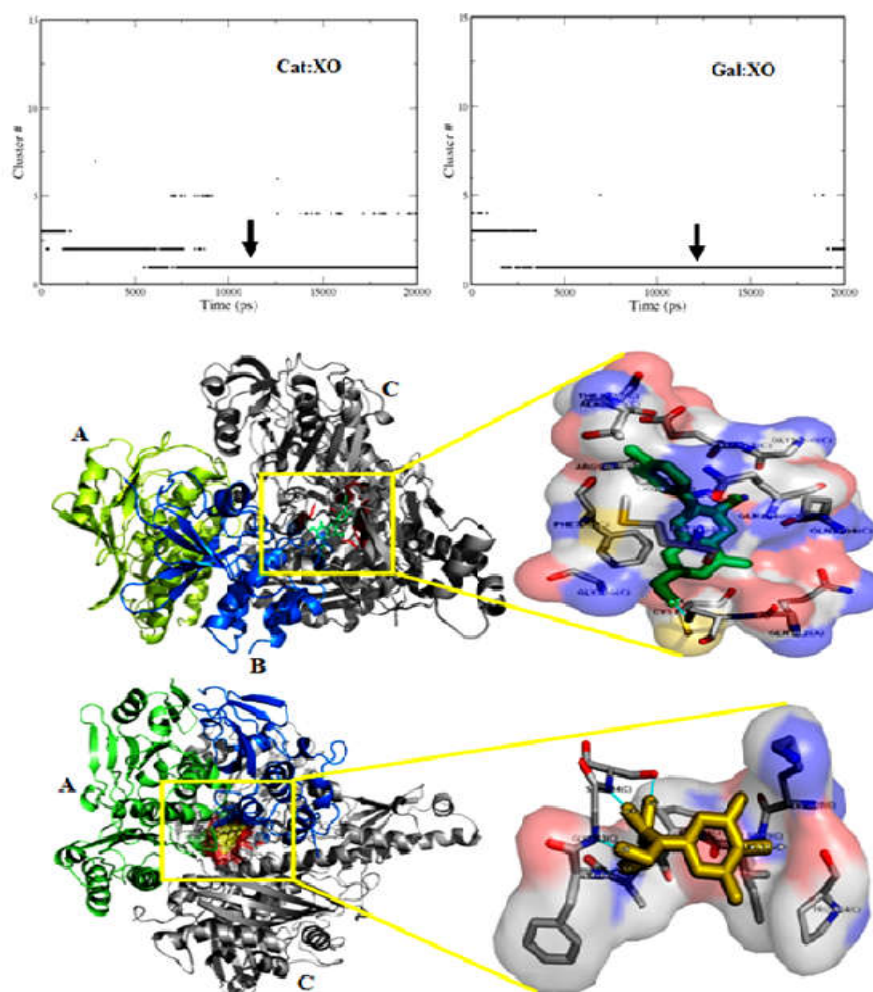


**Figure 6.8.** The size distribution of the clusters of the both complex, simulated for 20 ns. The temporal distribution is presented for each complex for backbone atoms, using the same cut-off value (0.15 nm). The arrow marks the number of clusters that encompass 95% of all structures. Cartoon visualization of representative structure (upper panel: cat: XO and lower: gal: XO), magnifying view depicts interacting residues within catechin  
*School of Biochemical Engineering, IIT(BHU) Varanasi*

(lime) and gallic-acid (yellow) surrounded by a surface of the electrostatic potential, depicting as red (negative potential) and blue (positive potential). Cyan line shows hydrogen bonding.

clusters and last one was showing longer lifetime, which was noted more than ~10-ns (bold arrow **Figure 6.8**). Both complexes were executed less noisy a smooth continuous trajectories of transition to a new conformation. The largest cluster is denoted by the bold arrow in figure 18, was used as a representative structure of cluster that was visualized for further illustration of binding residues in an electrostatic potential shell.

The cartoon representation of complex structures of the largest cluster of both approximations was offered a location of catechin and gallic-acid ligand and the enlarge view provides insight into the interaction residues and number of hydrogen bonds, which were formed during simulation. The electrostatic potential surface exhibits red, blue and white interface, a major negative lobe (red), a smaller positive one (blue) and neutral (white). The electrostatic interface of XO's surface indicates a total electrostatic area of interaction with ligand. In case of catechin the interacting amino acid residues, which were covered mostly positive potential, however, negative lobe was also occupied by some residues. Whereas, due to lesser molecular weight, gallic-acid, the binding amino acid residues were covered less surface area. Mostly neutral (white) electrostatic lobe was found within binding pocket of gallic-acid. This presentation was fairly approximated by the level of  $4 k_B T$  surface (**Figure 6.8**), and bound to the protein, where ligands are trapped within deep energetic wells.

## 6.4. Conclusion

Antioxidant activity may be due to combined effects of all the phytochemicals constituents such as alkaloids, flavonoids, proteins, reducing sugars, steroids, terpenoids, or acting separately may be responsible for such activity. Molecular docking studies and

*in vitro* xanthine oxidase inhibitory activity revealed that polyphenols inhibited xanthine oxidase having more negative binding energy with respect to a synthetic drug such as allopurinol. Molecular docking described the probable binding poses with considerable binding energy, and the molecular dynamics simulations provided support of ligand's effect (catechin and gallic-acid), in the active site of XO. Catechin and gallic-acid are mostly trapped within the binding site and strictly bound with interacting residues within an appropriate electrostatic shell. The representative structure of the largest cluster was illustrated about both complexes which hold longer lifetime. These experimental outcomes indicated that faba bean (*Vicia faba* L.) polyphenols showed strong antioxidant and anti-gout properties and might be used as potential natural drugs against oxidative diseases.